Long noncoding RNA *SPRY4-IT1* regulates intestinal epithelial barrier function by modulating the expression levels of tight junction proteins

Lan Xiao[a,b], Jaladanki N. Rao[a,b], Shan Cao[c], Lan Liu[a,b], Hee Kyoung Chung[a,b], Yun Zhang[a,b], Jennifer Zhang[a,b], Yulan Liu[c], Myriam Gorospe[d], and Jian-Ying Wang[a,b,e,*]

[a]Cell Biology Group, Department of Surgery, and [e]Department of Pathology, University of Maryland School of Medicine, Baltimore, MD 21201; [b]Baltimore Veterans Affairs Medical Center, Baltimore, MD 21201; [c]Department of Gastroenterology, People's Hospital, Peking University, Beijing 100044, China; [d]Laboratory of Genetics, National Institute on Aging–Intramural Research Program, National Institutes of Health, Baltimore, MD 21224

ABSTRACT **Epithelial cells line the intestinal mucosa and form an important barrier to a wide array of noxious substances in the lumen. Disruption of the barrier integrity occurs commonly in various pathologies. Long noncoding RNAs (lncRNAs) control diverse biological processes, but little is known about the role of lncRNAs in regulation of the gut permeability. Here we show that the lncRNA *SPRY4-IT1* regulates the intestinal epithelial barrier function by altering expression of tight junction (TJ) proteins. *SPRY4-IT1* silencing led to dysfunction of the epithelial barrier in cultured cells by decreasing the stability of mRNAs encoding TJ proteins claudin-1, claudin-3, occludin, and JAM-1 and repressing their translation. In contrast, increasing the levels of *SPRY4-IT1* in the intestinal mucosa protected the gut barrier in mice exposed to septic stress by increasing the abundance of TJ proteins. *SPRY4-IT1* directly interacted with TJ mRNAs, and this process was enhanced through the association with the RNA-binding protein HuR. Of interest, the intestinal mucosa from patients with increased gut permeability exhibited a decrease in the levels of *SPRY4-IT1*. These findings highlight a novel role for *SPRY4-IT1* in controlling the intestinal epithelial barrier and define a mechanism by which *SPRY4-IT1* modulates TJ expression by altering the stability and translation of TJ mRNAs.**

Monitoring Editor
Thomas M. Magin
University of Leipzig

Received: Oct 13, 2015
Revised: Dec 8, 2015
Accepted: Dec 9, 2015

INTRODUCTION

Mammalian genomes transcribe a large number of noncoding RNAs with active roles in gene regulation (Ponting *et al.*, 2009). Long noncoding RNAs (lncRNAs) are defined as transcribed RNAs spanning >200 nucleotides in length that lack protein-coding potential, although many of them display several mRNA-like properties, including transcription from multiexonic genes and the presence of a 5′ cap and a 3′ poly(A) tail (Mattick *et al.*, 2006; Ulitsky *et al.*, 2013). Some lncRNAs are ubiquitous, but others can be expressed with tissue-, differentiation stage–, and cell type–specific expression patterns (Batista *et al.*, 2013). In addition, lncRNAs can regulate gene expression at different levels (Wang *et al.*, 2011); for example, some lncRNAs can remodel chromatin, recruit transcriptional activators or repressors, assemble ribonucleoprotein (RNP) complexes, serve as decoys that titrate away RNA-binding proteins (RBPs), and function as scaffolds for protein assembly (Ponting *et al.*, 2009; Batista *et al.*, 2013; Ulitsky *et al.*, 2013). Yet other lncRNAs can modulate gene expression by altering the stability and translation of mRNAs and working jointly with microRNAs (miRNAs) and RBPs (Wapinski *et al.*, 2011; Yoon *et al.*, 2012; Ulitsky *et al.*, 2013). Collectively lncRNAs

This article was published online ahead of print in MBoC in Press (http://www.molbiolcell.org/cgi/doi/10.1091/mbc.E15-10-0703) on December 17, 2015.

The authors declare no conflicts of interest.

*Address correspondence to: Jian-Ying Wang (jwang@smail.umaryland.edu).

Abbreviations used: AHA, L-azidohomoalanine; CUGBP1, CUG-binding protein 1; IEC, intestinal epithelial cell; lncRNA, long noncoding RNA; IP, immunoprecipitation; miRNA, microRNA; RBP, RNA-binding protein; RNP, ribonucleoprotein; siHuR, siRNA targeting HuR; UTR, untranslated region.

have been involved in a variety of cellular functions, physiological processes, and disease states (Tsai *et al.*, 2011; Liu *et al.* 2012; Abdelmohsen *et al.*, 2014; Takahashi *et al.*, 2014; Uchida *et al.*, 2015).

Epithelial cells line the intestinal mucosa and form an important barrier to a wide array of noxious substances in the lumen. The effectiveness and stability of the epithelial barrier depend on specialized structures composing different intercellular junctions, including tight junctions (TJs) and adherens junctions (AJs; Turner, 2009; Yang *et al.*, 2014). The TJ is the apicalmost element of the junctional complex and seals intestinal epithelial cells (IECs) together in a way that prevents even small molecules from leaking between cells (Schneeberger *et al.*, 2004; Turner, 2009). Four classes of TJ-transmembrane proteins and >30 TJ membrane–associated proteins have been identified in mammalian epithelial and endothelial cells (Schneeberger *et al.*, 2004; Furuse *et al.*, 2014). TJ complexes primarily consist of transmembrane proteins, such as occludin, tricellulin, and one or more members of the claudin family; these proteins also associate with a cytosolic plaque of TJ proteins such as ZO-1 that links tightly to the cortical cytoskeleton. TJs are highly dynamic, and their constituent proteins undergo continuous remodeling and turnover under tight regulation by numerous extracellular and intracellular factors. The dynamic maintenance of TJ protein levels is critical for normal function of the epithelial barrier, whereas disruption of TJ expression results in gut epithelial barrier dysfunction (Chen *et al.*, 2008; Turner, 2009; Yang *et al.*, 2014). Previous studies from our laboratory (Yu *et al.*, 2011, 2013; Zhuang *et al.*, 2013) and others (Ye *et al.*, 2011; Sharma *et al.*, 2013; Zhou *et al.*, 2015) have shown that the RBP HuR and miRNAs (such as miR-29, miR-192, and miR-195) modulate the stability and translation of mRNAs encoding TJ proteins and play an important role in the control of intestinal epithelial TJ permeability. However, the exact roles of lncRNAs in the regulation of TJ expression and gut permeability have not been elucidated.

The lncRNA *SPRY4-IT1* was originally identified as a 706–base pair transcript present in a large-scale study involving sequencing of adipose tissue cDNA (Qta *et al.*, 2004) and was further shown to be broadly expressed in various human tissues, including the intestinal mucosa (Khaitan *et al.*, 2011). *SPRY4-IT1* is derived from the intronic region of the *SPRY4* gene, but *SPRY4* mRNA and *SPRY4-IT1* are independent transcripts (Khaitan *et al.*, 2011; Mazar *et al.*, 2014). Expression of *SPRY4-IT1* is up-regulated in human melanoma cells and predominantly localized in cytoplasmic polysomes or ribosomal clusters (Ingolia *et al.*, 2012; Mazar *et al.*, 2014). Inhibition of *SPRY4-IT1* expression causes defects in cell proliferation and differentiation and induces apoptosis in melanoma cells, suggesting that it is implicated in melanocytic transformation (Khaitan *et al.*, 2011; Mazar *et al.*, 2014). Here we report a novel function for *SPRY4-IT1* in protecting the intestinal epithelial barrier function by enhancing TJ expression posttranscriptionally. Because *SPRY4-IT1* expression levels decrease in patients with increased gut permeability, our findings provide a strong rationale for developing new therapeutic strategies directed at *SPRY4-IT1* to preserve the integrity of the gut epithelial barrier in various pathological conditions.

RESULTS

SPRY4-IT1 is essential for normal function of the intestinal epithelial barrier in vitro

SPRY4-IT1 was highly expressed in IECs and distributed in both the cytoplasm and nucleus (Figure 1A), whereas the lncRNA *HULC* was localized only in the nucleus, as measured by confocal fluorescence analysis of optical sections and quantitative real-time PCR (Q-PCR) analysis (Supplemental Figure S1A). To identify the role of *SPRY4-IT1* in the regulation of intestinal epithelial barrier function, we silenced expression of *SPRY4-IT1* by transfecting Caco-2 cells with a specific small interfering RNA (siRNA) targeting *SPRY4-IT1* (siSPRY4-IT1). As shown in Figure 1B, the levels of total and cytoplasmic *SPRY4-IT1* decreased dramatically in siSPRY4-IT1-transfected cells compared with cells transfected with control siRNA (C-siRNA). Decreased levels of *SPRY4-IT1* by siSPRY4-IT1 transfection specifically inhibited expression of TJ proteins claudin-1, claudin-3, JAM-1, and occludin but failed to alter the cellular abundance of TJ protein ZO-1, AJ proteins E-cadherin, α-catenin, or β-catenin, and RBP HuR (Figure 1C). The levels of claudin-1, claudin-3, JAM-1, and occludin proteins in SPRY4-IT1–silenced cells decreased by ~95, ~96, ~93, and ~85% ($n = 3$; $p < 0.05$), respectively, compared with those in cells transfected with C-siRNA. To exclude off-target effects, we tested another siRNA targeting *SPRY4-IT1* (SPRY4-IT1-2), which showed a similarly repressive effect on the expression of *SPRY4-IT1*, as well as on this subset of TJ proteins (unpublished data). Consistent with this finding, *SPRY4-IT1* silencing also disrupted the epithelial barrier function in an in vitro model, as evidenced by a decrease in transepithelial electrical resistance (TEER) values (Figure 1D, top) and an increase in the levels of paracellular flux of fluorescein isothiocyanate (FITC)–dextran (Figure 1D, bottom). Moreover, the barrier dysfunction induced by silencing *SPRY4-IT1* was rescued by overexpression of TJ proteins, since decreased TEER and increased paracellular permeability were completely prevented when *SPRY4-IT1*–silenced cells were transfected with the claudin-1 or occludin expression vector (Figure 1E and Supplemental Figure S1). On the other hand, *SPRY4-IT1* silencing did not affect cell viability, as measured by trypan blue staining (unpublished data), and failed to alter Caco-2 cell proliferation, as determined by the lack of significant differences in the expression levels of proliferation-associated proteins (CDK4, 14-3-3, and CUG-binding protein 1 [CUGBP1]) and the numbers of cells in SPRY4-IT1–silenced populations and C-siRNA cells (Supplemental Figure S2). We also examined changes in TJ expression after ectopic overexpression of *SPRY4-IT1* and found that transfection of cells with the *SPRY4-IT1* expression vector marginally increased expression levels of claudin-1 and occludin but did not affect claudin-3 or JAM-1 content (Supplemental Figure S3). In addition, neither TJ expression nor epithelial barrier function was affected by ectopic overexpression or silencing of lncRNA *HULC* (unpublished data). These data indicate that *SPRY4-IT1* is necessary for normal expression of given TJ proteins and maintaining epithelial barrier function but not for increasing the basal levels of TJ proteins.

Elevation of *SPRY4-IT1* protects the gut barrier function in mice exposed to septic stress

In an effort to define the in vivo importance of *SPRY4-IT1* in regulating gut barrier function, we increased the levels of *SPRY4-IT1* by infecting mice with the recombined *SPRY4-IT1* lentiviral expression vector (lenti-SPRY4-IT1) as described previously (Scherr *et al.*, 2007; Feng *et al.*, 2012). Briefly, lenti-SPRY4-IT1 containing expressed *SPRY4-IT1*/GFP was under the control of the suCMV-promoter (AMSBIO, Cambridge, MA). As shown in Figure 2A, in situ detection in the mucosa of the small intestine showed a predominant accumulation of the lenti-SPRY4-IT1 in the villous area in mice infected with lenti-SPRY4-IT1 for 7 d. Minor FITC signal of the lenti-SPRY4-IT1 was also observed in the crypt area of the mucosa. By 7 d after infection with lenti-SPRY4-IT1, there was a sustained increase (~3.2-fold) in *SPRY4-IT1* in the intestinal mucosa (Figure 2B) compared with the levels in animals infected with the control

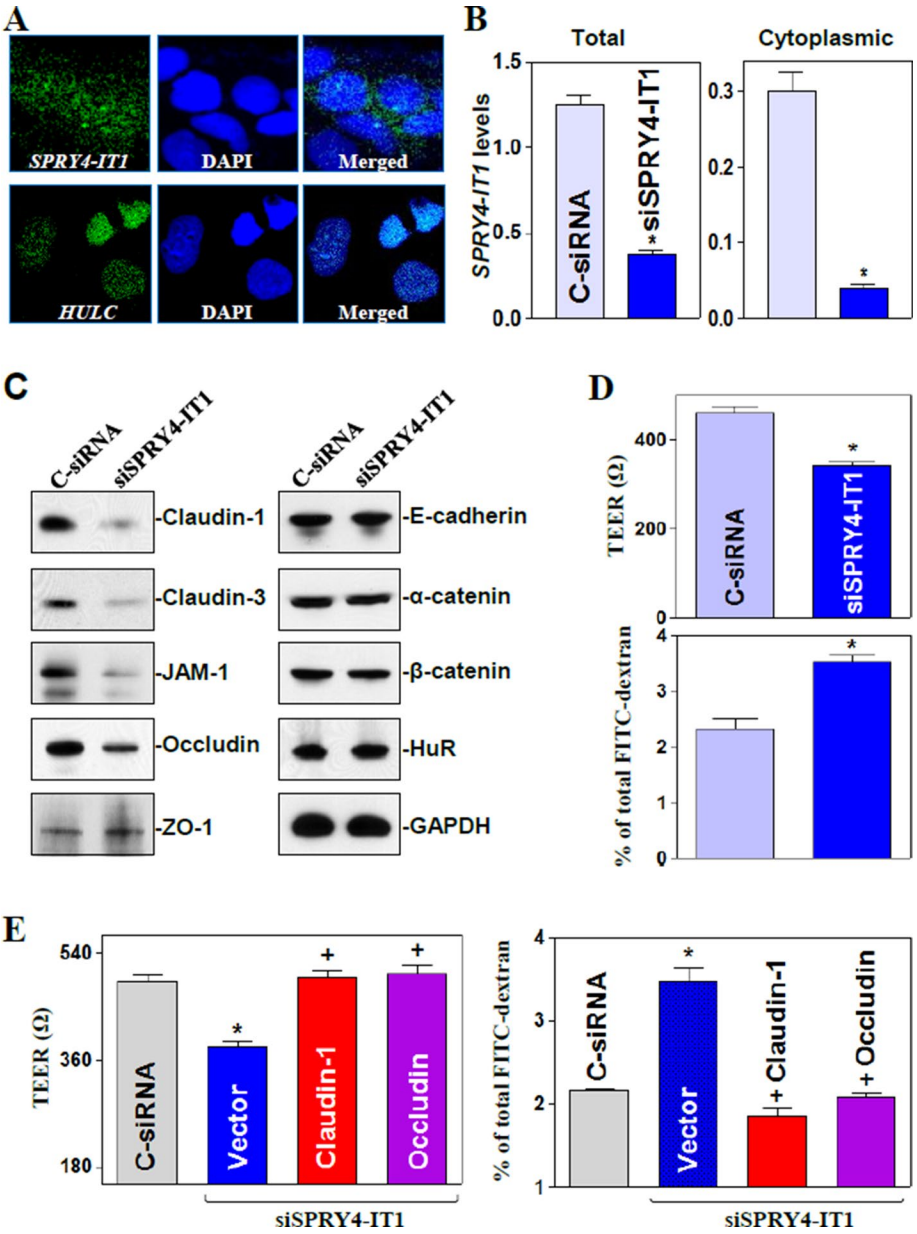

FIGURE 1: SPRY4-IT1 silencing inhibits TJ expression and disrupts the epithelial barrier function. (A) Cellular distribution of lncRNAs *SPRY4-IT1* (top) and HULC (bottom) in Caco-2 cells as measured by FISH assays. (B) Levels of total (left) and cytoplasmic (right) *SPRY4-IT1* 48 h after transfecting cells with siRNA targeting *SPRY4-IT1* (siSPRY4-IT1) or control siRNA (C-siRNA). Values are means ± SEM from three separate experiments. *$p < 0.05$ compared with C-siRNA. (C) Representative immunoblots of tight junctions and adherens junctions in cells described in B. (D) Changes in epithelial barrier function as indicted by changes in TEER (top) and FITC-dextran paracellular permeability (bottom) after SPRY4-IT1 silencing. (E) Ectopic TJ overexpression rescues the barrier dysfunction in SPRY4-IT1–silenced cells. Cells were cotransfected with siSPRY4-IT1 and the claudin-1 or occludin expression vector; TEER and FITC-dextran permeability were examined 48 h thereafter. *,+$p < 0.05$ compared with C-siRNA or siSPRY4-IT1 alone, respectively.

lentiviral vector (C-lentiviral). RNA fluorescence in situ hybridization (RNA-FISH) analysis revealed that increased *SPRY4-IT1* in the mucosa was localized at both villus and crypt areas (Figure 2C). To define the major cell type(s) present in the tissue extracted in these preparations, fluorescence-activated cell sorting analysis was performed as described previously (Terahara *et al.*, 2008; Nagatake *et al.*, 2014). As shown in Supplemental Figure S4, ~90% of the cell population in the extracted intestinal mucosa scraped using a glass microscope slide were intestinal epithelial cells.

Consistent with the findings observed in in vitro experiments, overexpression of *SPRY4-IT1* by infection with lenti-SPRY4-IT1 did not alter basal expression levels of TJ proteins or gut permeability (Figure 2, D and E, left) in control mice (sham groups). To test whether *SPRY4-IT1* overexpression enhanced the gut barrier function under critical pathological conditions, we subjected the mice to septic stress using the cecal ligation and puncture (CLP) model (Hubbard *et al.*, 2005). Exposure to CLP for 24 h caused an acute gut barrier dysfunction in both C-lentiviral– and lenti-SPRY4-IT1–infected mice, as indicated by an increase in gut mucosal permeability to FITC-dextran. Of interest, however, gut permeability induced by CLP was significantly lower in mice infected with lenti-SPRY4-IT1 than in mice infected with C-lentiviral (Figure 2D, right). As expected, CLP stress also decreased the levels of TJ proteins claudin-1, claudin-3, occludin, and JAM-1 in the intestinal mucosa, but the inhibition of TJ protein expression by CLP was almost completely prevented or significantly reduced by increasing the levels of *SPRY4-IT1* in lenti-SPRY4-IT1-infected mice (Figure 2E, right). On the other hand, there were no significant changes in histological features of the small intestinal mucosa between C-lentiviral–infected mice and mice infected with lenti-SPRY4-IT1 with or without CLP-induced stress (Figure 2F). These results indicate that increasing the levels of intestinal mucosal *SPRY4-IT1* protects the barrier function against CLP-induced stress by derepressing TJ protein expression.

SPRY4-IT1 stabilizes TJ mRNAs and enhances their translation

To investigate the mechanism underlying *SPRY4-IT1* in regulating TJ expression, we examined changes in the stability and translation of TJ mRNAs after SPRY4-IT1 silencing. Knockdown of *SPRY4-IT1* expression by transfection with siSPRY4-IT1 decreased the levels of *claudin-1*, *occludin*, *claudin-3*, and *JAM-1* mRNAs (Figure 3A) by increasing their degradation rates. The half-lives of these TJ mRNAs in the SPRY4-IT1–silenced population of cells were decreased compared with those in cells transfected with C-siRNA (Figure 3B). However, quantitative analysis of these results indicated that the levels of TJ protein expression were decreased by >80% in SPRY4-IT1-silenced cells (Figure 1C), whereas the levels of the respective TJ mRNAs were reduced by only ~25–40%.

Therefore we investigated the involvement of *SPRY4-IT1* in the regulation of TJ translation. De novo TJ protein synthesis after

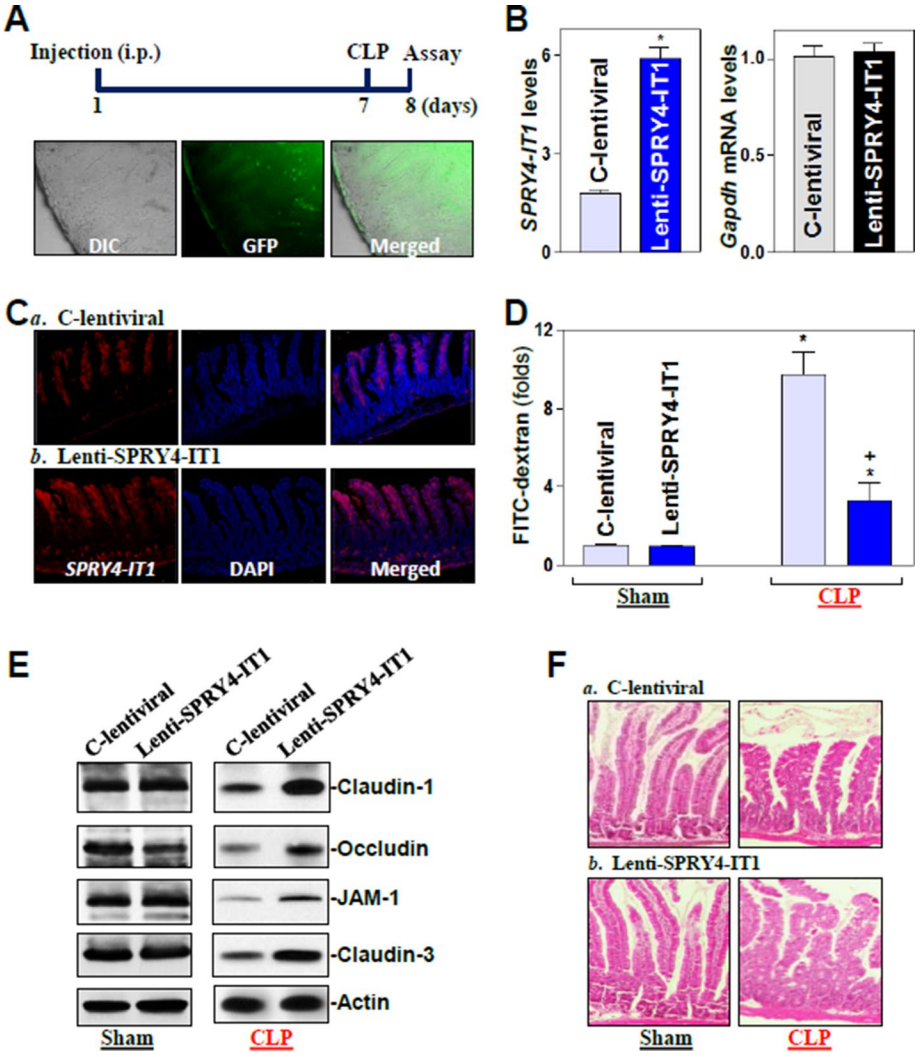

FIGURE 2: Elevation of mucosal *SPRY4-IT1* by infection with a *SPRY4-IT1* lentiviral expression vector protects gut TJ barrier function in mice exposed to CLP. (A) Distribution of the lenti-SPRY4-IT1 (GFP) in the small intestinal mucosa 7 d after intraperitoneal (i.p.) injection. (B) Levels of *SPRY4-IT1* in the small intestinal mucosa in mice described in A. Values are means ± SEM ($n = 4$). *$p < 0.05$ compared with C-control lentiviral vector (C-lentiviral). (C) Distribution of *SPRY4-IT1* in the small intestine as measured by FISH in mice described in A. (D) Gut permeability in sham mice and mice exposed to CLP for 24 h. FITC-dextran was given orally, and blood samples were collected 4 h later. *,+$p < 0.05$ compared with sham or C-lentiviral-treated mice exposed to CLP, respectively. (E) Representative immunoblots of tight junctions in the small intestinal mucosa in mice described in D. (F) Hematoxylin/eosin staining of the intestinal mucosa.

SPRY4-IT1 silencing was analyzed by measuring L-azidohomoalanine (AHA) incorporation. We found that the levels of newly synthesized claudin-1, clauidn-3, occludin, and JAM-1 proteins in siSPRY4-IT1–transfected cells decreased by ~75, ~90, ~85, and ~90% ($n = 3$; $p < 0.05$), respectively, compared with the levels in cells transfected with C-siRNA (Figure 3C). Inhibition of synthesis of these TJ proteins by *SPRY4-IT1* silencing was specific, since there was no change in nascent glyceraldehyde-3-phosphate dehydrogenase (GAPDH) synthesis in siSPRY4-IT1–transfected cells. Changes in translation of these proteins were further studied by measuring the sizes of polysomes after silencing *SPRY4-IT1*. We fractionated cytoplasmic components through sucrose gradients and analyzed polysome distribution profiles. Although decreasing the levels of *SPRY4-IT1* did not affect global polysomal profiles (unpublished data), the abundance of each of TJ mRNAs associated with actively translating fractions (peaking at fraction 9) decreased in siSPRY4-IT1–transfected cells, with a moderate leftward shift of the mRNAs toward lower-translating fractions (peaking at fraction 8; Figure 3D). In contrast, *Gapdh* mRNA, encoding a housekeeping protein, was distributed similarly in both groups. These results indicate that *SPRY4-IT1* induces TJ levels by both stabilizing TJ mRNAs and enhancing their translation.

SPRY4-IT1 is required for HuR binding to and also directly interacts with TJ mRNAs

HuR bound the 3′-untranslated regions (UTRs) of *claudin-1* and *occludin* mRNAs and enhanced their translation and stability (Yu *et al.*, 2011; Sharma *et al.*, 2013). The *claudin-3* and *JAM-1* mRNAs are also potential targets of HuR, as they contain computationally predicted HuR-binding sites in their 3′-UTRs. Because both HuR and *SPRY4-IT1* regulate TJ expression at the posttranscriptional level, we tested the possibility that *SPRY4-IT1* alters the association of HuR with the TJ mRNAs. To do so, we synthesized biotin-labeled *SPRY4-IT1* and examined the direct interaction of *SPRY4-IT1* with HuR in an in vitro system. Cytoplasmic lysates were initially incubated with biotinylated *SPRY4-IT1* as described previously (Cao *et al.*, 2014), and then the levels of HuR and other proteins in the pull-down material were assessed by Western blot analysis. As shown in Figure 4A, biotinylated *SPRY4-IT1* specifically bound to HuR but did not bind other RBPs, such as CUGBP1 (also named as CELF1), TIAR, or AUF1, as determined by biotin pull-down analysis. *SPRY4-IT1* also failed to directly interact with TJ proteins claudin-1, claudin-3, occludin, and JAM-1. To examine further the association of endogenous *SPRY4-IT1* with endogenous HuR, we performed RNP immunoprecipitation (IP) using anti-HuR antibody and control immunoglobulin G (IgG), followed by isolation of bound RNA in both IP reactions. After reverse transcription (RT), Q-PCR analysis was used to measure the levels of *SPRY4-IT1* enrichment in the HuR IP relative to IgG IP, as previously described (Zou *et al.*, 2010). *SPRY4-IT1* was highly enriched in HuR IP compared with control IgG IP (Figure 4Ba). In contrast, there were no significant changes in the levels of lncRNAs *HULC* and *PTENP1* in HuR IP samples. As anticipated, the levels of TJ mRNAs, including *claudin-1*, *claudin-3*, *occludin*, and *JAM-1* mRNAs but not *ZO-1* mRNA, were also highly enriched in HuR IP samples (Figure 4Bb). HuR/*SPRY4-IT1* association did not affect the stability of *SPRY4-IT1*, since HuR silencing by transfection with siRNA specifically targeting HuR (siHuR) did not alter cellular *SPRY4-IT1* levels or its half-life (Supplemental Figure S5). Of interest, *SPRY4-IT1* silencing by transfecting cells with siSPRY4-IT1 blocked HuR binding to *claudin-1*, *claudin-3*, *occludin*, and *JAM-1* mRNAs (Figure 4C), although it did not affect total HuR abundance or its

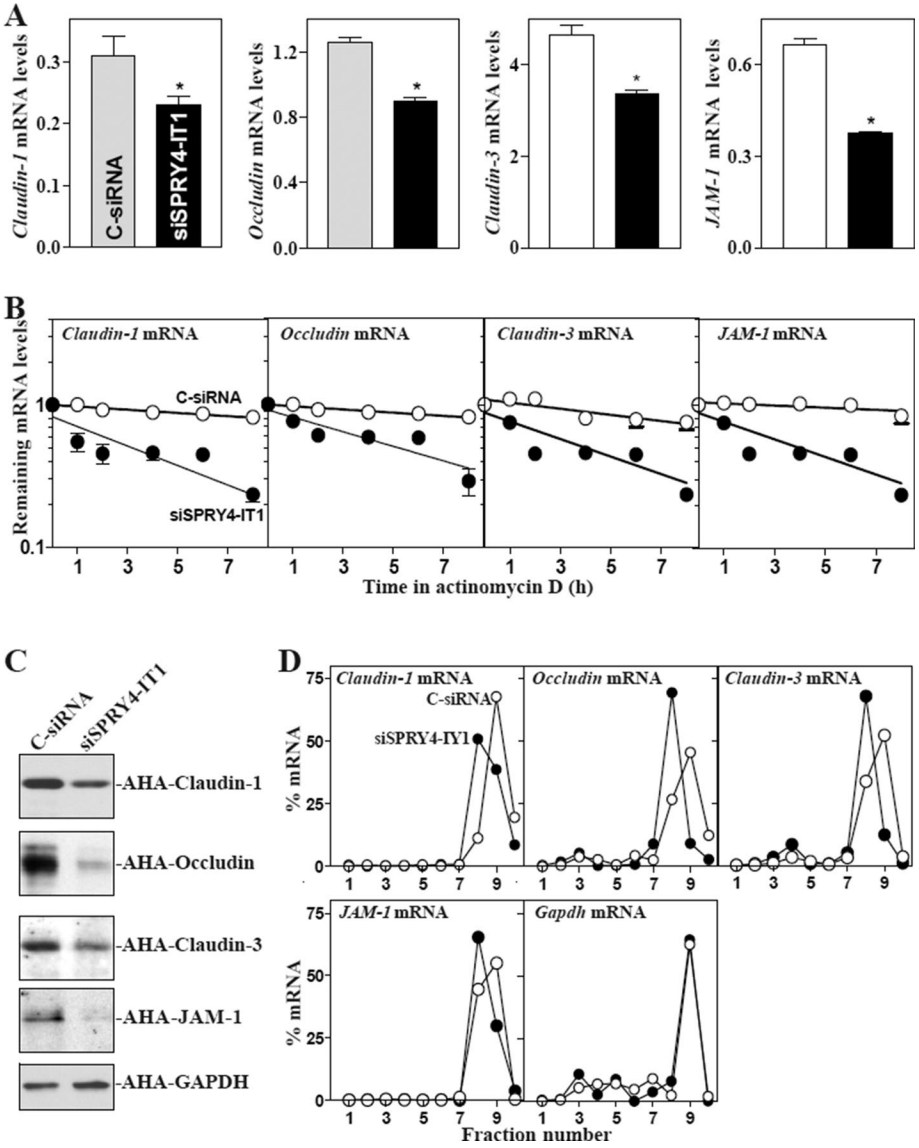

FIGURE 3: SPRY4-IT1 silencing enhances TJ mRNA decay and represses their translation. (A) Levels of *claudin-1*, *occludin*, *claudin-3*, and *JAM-A* mRNAs 48 h after transfection with siSPRY4-IT1 or C-siRNA. Values are means ± SEM from three separate experiments. *$p < 0.05$ compared with C-siRNA. (B) Stability of the TJ mRNAs in cells described in A. mRNA levels were examined at different times after administration with actinomycin D. (C) Newly synthesized TJ proteins in SPRY4-IT1–silenced cells. After cells were exposed to AHA, cell lysates were incubated with the reaction buffer containing biotin/alkyne reagent; the biotin-alkyne/azide–modified protein complex was pulled down by paramagnetic streptavidin-conjugated Dynabeads. (D) Distribution of *claudin-1*, *occludin*, *claudin-3*, and *JAM-A* mRNAs in each gradient fraction prepared from polysomal profile after SPRY4-IT1 silencing. Nuclei were pelleted, and the resulting supernatants were fractionated through a 10–50% linear sucrose gradient. Total RNA was isolated from different fractions, and the levels of TJ and *Gapdh* mRNAs were measured and plotted as a percentage of each of total TJ mRNAs and *Gapdh* mRNA levels in the samples. Three experiments were performed and showed similar results.

subcellular distribution (Supplemental Figure S6A). In contrast, silencing *SPRY4-IT1* had no effect on HuR association with the *Atf2* or *Jund* mRNAs (unpublished data).

There are multiple predicted *SPRY4-IT1*-binding sites in the 3′-UTRs of *claudin-1*, *claudin-3*, *occludin*, and *JAM-1* (Figure 5A and Supplemental Table S1). RNA–RNA pull-down assays showed that the levels of *claudin-1*, *claudin-3*, *occludin*, and *JAM-1* mRNAs were much higher in biotinylated *SPRY4-IT1* pull-down samples than those in biotin-labeled *Gapdh* pull-down samples (Figure 5B). Of interest, transfection of cells with siHuR almost completely depleted HuR levels (Supplemental Figure S6B) but only decreased rather than totally prevented the binding of *SPRY4-IT1* to *claudin-1*, *claudin-3*, *occludin*, and *JAM-1* mRNAs (Figure 5C), indicating that *SPRY4-IT1* also directly binds the TJ mRNAs and that this interaction is independent of its association with HuR. These findings strongly suggest a model in which *SPRY4-IT1* controls intestinal epithelial TJ permeability (Figure 5D): 1) *SPRY4-IT1* is essential for HuR binding to TJ mRNAs, 2) *SPRY4-IT1* also directly interacts with TJ mRNAs, and 3) *SPRY4-IT1*/TJ mRNA associations stabilize and enhance TJ mRNA translation, thus increasing TJ protein production and promoting the function of the epithelial barrier.

Decreased expression of *SPRY4-IT1* in patients with increased gut permeability

To study the effect of *SPRY4-IT1*–regulated TJ expression on clinical conditions, we examined changes in the levels of *SPRY4-IT1* in human intestinal mucosa from patients with increased gut permeability. The colonic mucosal tissues in patients with ulcerative colitis, who were diagnosed with increased gut permeability clinically, were collected for measurements of *SPRY4-IT1* levels and TJ expression, with the mucosal samples from patients without significant changes in gut permeability serving as controls. As shown in Figure 6A, *SPRY4-IT1* levels in the mucosa obtained from patients with increased gut permeability were significantly lower than those measured in control patients. The reduced *SPRY4-IT1* expression levels in patients with increased gut permeability were further confirmed by RNA-FISH analysis, which revealed a decrease in *SPRY4-IT1* fluorescence intensity in the mucosa (Figure 6B). Consistent with our findings from cultured IECs (Figure 1) and mice (Figure 2), decreased levels of *SPRY4-IT1* in all of the patients we examined were correlated with an inhibition of TJ expression, as shown by a decrease in claudin-1, claudin-3, occludin, and JAM-1 immunostaining (Figure 6C). These results suggest that decreased *SPRY4-IT1* and subsequent inhibition of TJ expression contribute to the pathogenesis of gut barrier dysfunction in patients.

DISCUSSION

Acute gut barrier dysfunction occurs commonly in certain pathological conditions. It can lead to the translocation of toxic substances and bacteria from the intestinal lumen to the bloodstream, and in extreme cases it can result in multiple organ dysfunction

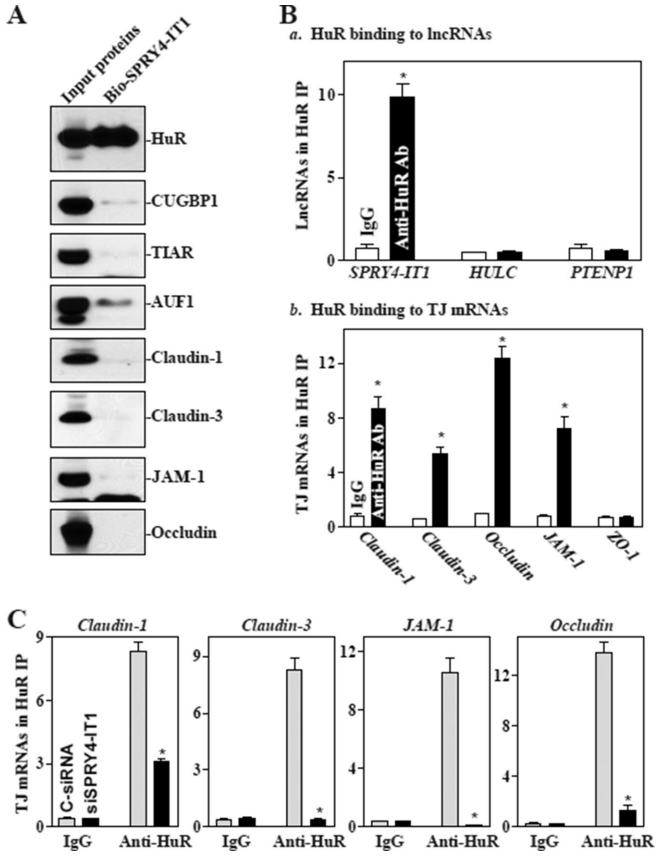

FIGURE 4: *SPRY4-IT1* is essential for HuR interaction with TJ mRNAs. (A) *SPRY4-IT1* directly binds to HuR but not to other RBPs and TJ proteins. After cytoplasmic lysates were incubated with biotinylated *SPRY4-IT1*, levels of HuR and other proteins in the pull-down material were assessed. (B) Association of endogenous HuR with endogenous *SPRY4-IT1* (a) and TJ mRNAs (b). After IP of RNA–protein complexes from cell lysates using anti-HuR antibody (Ab) or control IgG1, RNA was isolated and measured by Q-PCR analysis. Values are means ± SEM from three separate experiments. *$p < 0.05$ compared with IgG. (C) SPRY4-IT1 silencing represses HuR association with TJ mRNAs. Forty-eight hours after cells were transfected with siSPRY4-IT1 and C-siRNA, the association of HuR with TJ mRNAs was measured. *$p < 0.05$ compared with C-siRNA.

syndrome and death (Zhang *et al.*, 2010; Carter *et al.*, 2013). Because the exact mechanism responsible for increased gut permeability is obscure, effective therapies to preserve the integrity of the epithelial barrier are limited, especially in surgical intensive care patients supported with total parenteral nutrition (Mosenthal *et al.*, 2002; Carter *et al.*, 2013). Identification of the underlying causes and successful medical treatment are major challenges, and efforts to develop effective therapeutics to protect the barrier function are extremely important. Here we identify a novel mechanism by which the lncRNA *SPRY4-IT1* controls intestinal epithelial barrier function by altering TJ expression and further show that *SPRY4-IT1* regulates TJ levels primarily at the posttranscriptional level. Knockdown of *SPRY4-IT1* expression caused epithelial barrier dysfunction as a result of inhibition of TJ expression in vitro, whereas increased levels of *SPRY4-IT1* in the intestinal mucosa not only prevented CLP-induced TJ repression, but they also protected the gut epithelial barrier against septic stress in vivo. These findings are a significant conceptual advance by linking the lncRNA *SPRY4-IT1* with TJ expression and subsequent gut permeability and underscore the effect of *SPRY4-IT1* in the pathogenesis of acute gut barrier dysfunction.

SPRY4-IT1 is actively transcribed from an intron of the *SPRY4* gene and undergoes maturation by cleavage of the 5′ region in the nucleus before transport to the cytoplasm (Mazar *et al.*, 2014), and sequence analysis confirmed that *SPRY4-IT1* does not show any coding potential. Although *SPRY4-IT1* is expressed in different human tissues, our understanding of its biological function and involvement in pathology is limited. It has been reported that *SPRY4-IT1* is implicated in the molecular etiology of human melanoma, because decreasing the levels of *SPRY4-IT1* inhibits cell growth and induces apoptosis in melanoma cells (Khaitan *et al.*, 2011). Further study demonstrated that *SPRY4-IT1* binds to the lipid phosphatase lipin 2 and modulates apoptosis by altering lipin 2–mediated lipid metabolism (Mazar *et al.*, 2014). A recent study also showed that *SPRY4-IT1* stimulates proliferation of human breast cancer cells by up-regulating ZNF703 expression (Shi *et al.*, 2015). Our present results provide new evidence that *SPRY4-IT1* regulates the stability and translation of mRNAs encoding TJ proteins claudin-1, claudin-3, occludin, and JAM-1. Because *SPRY4-IT1* is associated with polyribosomes (Ingolia *et al.*, 2012; Mazar *et al.*, 2014), it is likely that *SPRY4-IT1* enhances TJ levels posttranscriptionally by increasing recruitment of these TJ mRNAs to polyribosomes. In support of this notion, our results show that *SPRY4-IT1* was enriched in actively translating fractions prepared from polysomal gradients (Supplemental Figure S7) and that *SPRY4-IT1* silencing caused a shift of TJ mRNAs from actively translating fractions to low-translating fractions of polyribosomes. Efforts are underway in our laboratory to understand the specific mechanisms by which *SPRY4-IT1* regulates the translation of TJ proteins and whether *SPRY4-IT1* might also modulate TJ gene transcription.

The results reported here also indicate that *SPRY4-IT1* interacts with HuR and that *SPRY4-IT1*/HuR associations are essential for HuR binding to the TJ mRNAs. HuR has three RNA recognition motifs through which it directly interacts with numerous mRNAs to modulate their translation and/or stability (Mukherjee *et al.*, 2011; Yoon *et al.*, 2012; Liu *et al.*, 2014). Through its effect on target mRNAs, HuR has been implicated in many aspects of cellular functions and human diseases (Srikantan *et al.*, 2012a). Our previous studies revealed that HuR functions as a master regulator of TJ expression in the intestinal epithelium and that inhibition of HuR expression or disruption of its binding affinity causes intestinal epithelial barrier dysfunction in vitro as well as in vivo (Yu *et al.*, 2011, 2013; Yang *et al.*, 2014; Xiao *et al.*, 2014). HuR also interacts with noncoding RNAs (ncRNAs) such as miRNAs and lncRNAs to jointly regulate target transcripts antagonistically or synergistically (Kim *et al.*, 2009; Liu *et al.*, 2009; Mukherjee *et al.*, 2011; Srikantan *et al.*, 2012b; Yoon *et al.*, 2012; Abdelmohsen *et al.*, 2014). For example, HuR binds *lncRNA-p21* and induces the recruitment of let-7/Ago to *lncRNA-p21*, leading to destabilization of *lncRNA-p21* (Yoon *et al.*, 2012); HuR also competes with ncRNA *7SL* to modulate p53 translation (Abdelmohsen *et al.*, 2014). In this study, although *SPRY4-IT1* silencing did not affect total HuR levels or subcellular distribution, it robustly decreased the levels of the TJ mRNAs encoding claudin-1, claudin-3, occludin, and JAM-1 in HuR IP materials (Figure 4C), indicating that *SPRY4-IT1* is required for HuR binding to these TJ mRNAs. On the other hand, the 3′-UTRs of all of these TJ mRNAs contain multiple predicted *SPRY4-IT1*-binding sites, and HuR silencing decreases but does not completely block *SPRY4-IT1* association with the TJ mRNAs, as measured by biotinylated *SPRY4-IT1* pull-down assays (Figure 5C), suggesting that *SPRY4-IT1* is also capable of interacting directly with TJ mRNAs independently of its interaction with HuR.

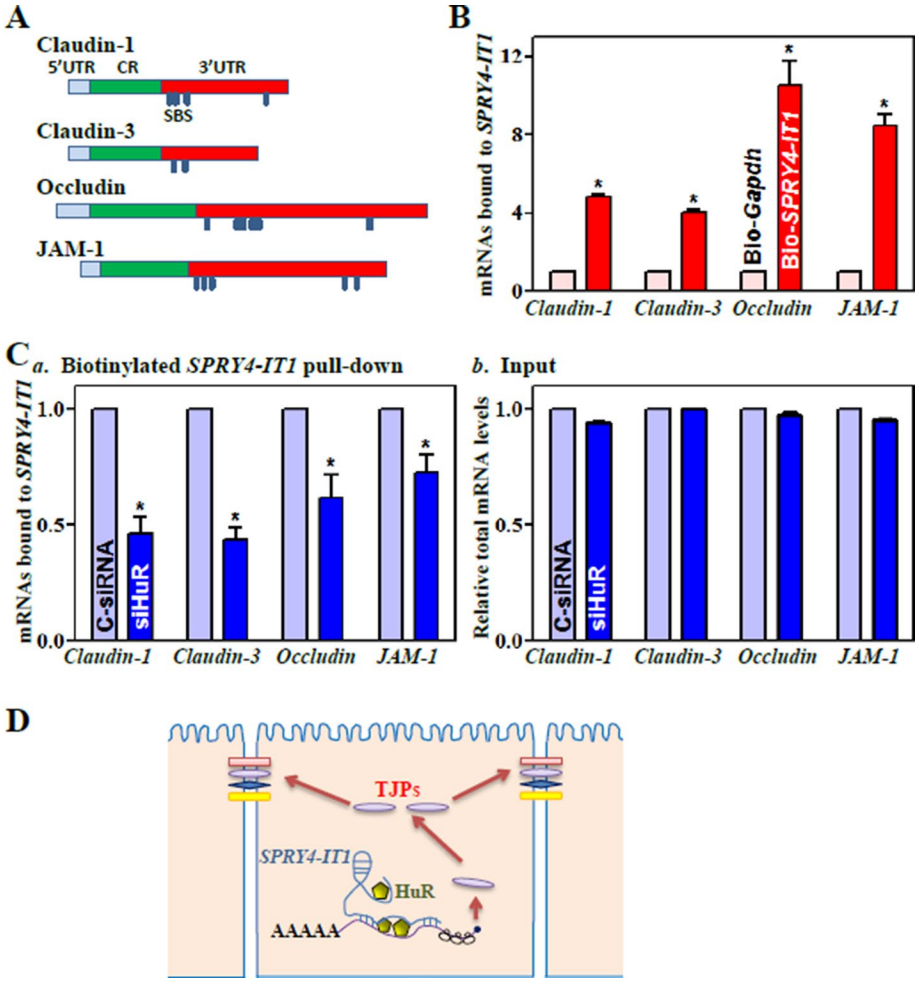

FIGURE 5: *SPRY4-IT1* directly interacts with TJ mRNAs. (A) Schematic of TJ mRNAs depicting potential binding sites of *SPRY4-IT1* in the 3′-UTRs of *claudin-1*, *claudin-3*, *occludin*, and *JAM-1* mRNAs. SBS, potential *SPRY4-IT1*-binding site. (B) *SPRY4-IT1* association with mRNAs encoding claudin-1, claudin-3, occludin, and JAM-1 as measured by using biotinylated *SPRY4-IT1*. Values are means ± SEM from three separate experiments. *$p < 0.05$ compared with biotin-labeled *Gapdh*. (C) Binding of biotinylated SPRY4-IT1 to TJ mRNAs after HuR silencing: (a) levels of *TJ* mRNAs in the materials pulled down by biotin-*SPRY4-IT1*, and (b) levels of total input mRNAs. Cells were transfected with siHuR or C-siRNA, and association of TJ mRNAs with *SPRY4-IT1* was measured 48 h thereafter. *$p < 0.05$ compared with C-siRNA. (D) Schematic of proposed influence of SPRY4-IT1 on the epithelial TJ permeability. *SPRY4-IT1* is essential for HuR binding to the TJ mRNAs and also directly interacts with the TJ mRNAs, thus enhancing TJ expression and barrier function.

Because patients with increased gut permeability displayed decreased levels of *SPRY4-IT1* in the gut mucosa, therapies aimed at systemically overexpressing *SPRY4-IT1* might enhance intestinal epithelial barrier function in specific clinical settings. Although the complete sets of mRNAs controlled by *SPRY4-IT1* and the underlying mechanism in the intestinal epithelium remain to be fully elucidated, the fact that overexpressing *SPRY4-IT1* using a lentivirus protected the gut barrier function in mice exposed to CLP highlights the effect of an individual lncRNA in controlling gut permeability. These findings are particularly significant in patients with traumatic damage, thermal injury, shock, and recovery from major surgical operations, as acute gut barrier dysfunction occurs commonly in these critical surgical conditions (Zhang *et al.*, 2010; Carter *et al.*, 2013).

Unlike most traditional therapeutics, in which drugs have specific cellular targets, modulating lncRNAs or miRNAs regulates entire functional gene networks (Wapinski *et al.*, 2011; Mendell *et al.*, 2012). Of course, this broad spectrum of actions should be pursued with caution, since unintended off-target effects may also occur. In sum, our results indicate that *SPRY4-IT1* is a potent biological regulator of the intestinal epithelial TJ permeability through its interaction with HuR. These findings can also potentially provide innovative molecular therapy to protect the gut epithelial barrier function in patients with various critical disorders.

MATERIALS AND METHODS

Cell culture and animals

The Caco-2 human colon carcinoma cell line was purchased from the American Type Culture Collection (Manassas, VA) and maintained in standard culture conditions (Chen *et al.*, 2008). Tissue culture medium and dialyzed fetal bovine serum were obtained from Invitrogen (Carlsbad, CA), and biochemicals were obtained from Sigma-Aldrich (St. Louis, MO). Antibodies recognizing claudin-1, claudin-3, occludin, ZO-1, HuR, and β-actin were obtained from Santa Cruz Biotechnology (Santa Cruz, CA) and BD Biosciences (Sparks, MD), and the secondary antibody conjugated to horseradish peroxidase was obtained from Sigma-Aldrich.

C57BL/65 mice (male and female, 6–9 wk old) were purchased from the Jackson Laboratory (Bar Harbor, ME) and housed in specific pathogen-free animal facility at the Baltimore VA Medical Center. All animal experiments were conducted in accordance with National Institutes of Health guidelines and were approved by the Institutional Animal Care and Use Committee of the University of Maryland School of Medicine and Baltimore VA Hospital.

Plasmid construction and RNA interference

Lenti-SPRY4-IT1 was custom made by AMS-BIO, in which *SPRY4-IT1*/GFP expression was under the control of the suCMV-promoter. Lenti-SPRY4-IT1 and C-lentiviral were packaged in lentiviral production cells, concentrated by ultracentrifugation, resuspended in phosphate-buffered saline (PBS), and used to increase *SPRY4-IT1* in vivo as described (Scherr *et al.*, 2007; Feng *et al.*, 2012). An expression vector containing SPRY4-IT1 cDNA under control of pCMV-promoter was constructed (Liu *et al.*, 2009) and used to increase *SPRY4-IT1* in Caco-2 cells; claudin-1 and occludin expression vectors were obtained from Origene (Rockville, MD).

Expression of *SPRY4-IT1* and HuR was silenced by transfection with specific siRNA as described (Cui *et al.*, 2011; Liu *et al.*, 2015). The siSPRY4-IT1, siHuR, and C-siRNA were purchased from Santa Cruz Biotechnology. For each 60-mm cell culture dish, 15 μl of the 20 μM stock duplex siSPRY4-IT1, siHuR, or C-siRNA was used. Forty-eight hours after transfection using Lipofectamine, cells were harvested for analysis.

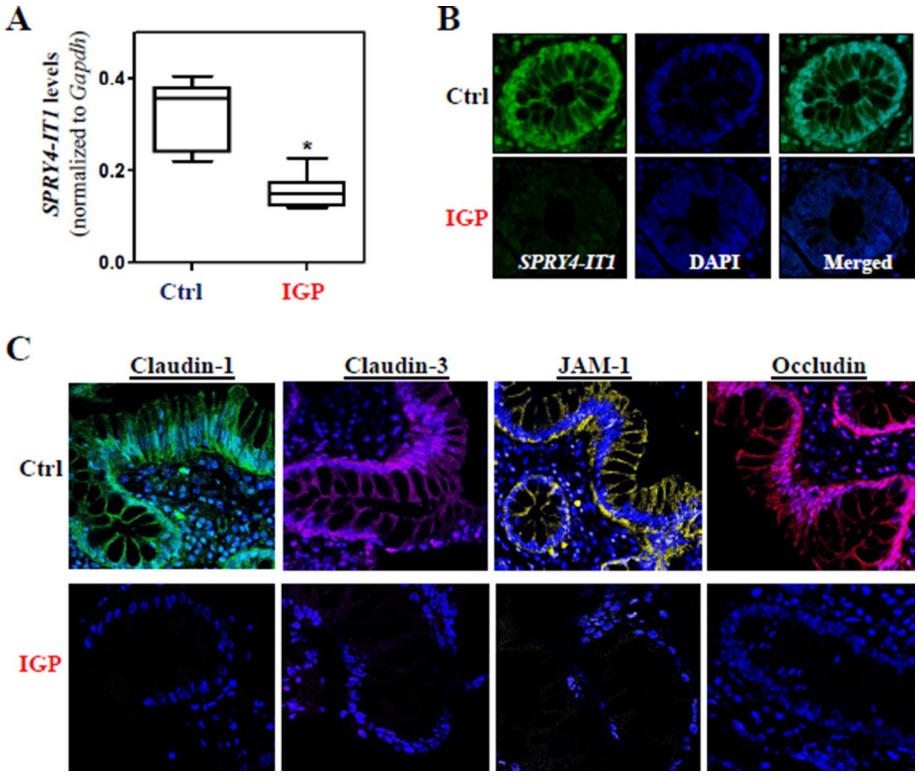

FIGURE 6: Association of decreased *SPRY4-IT1* with reduction in the levels of TJs in patients with gut barrier dysfunction. (A) Levels of *SPRY4-IT1* in the intestinal mucosa in patients with increased gut permeability (IGP) or controls (Ctrl) as measured by Q-PCR analysis and normalized to *Gapdh* levels. Values are means ± SEM ($n = 7$). *$p < 0.05$ compared with controls. (B) In situ hybridization of *SPRY4-IT1* with fluorescent LNA RNA detection probe in the intestinal mucosa described in A. (C) Immunohistochemical staining of TJ proteins in the intestinal mucosa described in A.

Quantitative real-time PCR and immunoblotting analyses

Total RNA was isolated by using the RNeasy minikit (Qiagen, Valencia, CA) and used in RT and PCR amplification reactions as described (Zou *et al.*, 2015). Q-PCR was performed using Step-one-plus Systems with specific primers, probes, and software (Applied Biosystems, Foster City, CA).

To examine protein levels, whole-cell lysates were prepared using 2% SDS, sonicated, and centrifuged at 4°C for 15 min. The supernatants were boiled for 5 min and size fractionated by SDS–PAGE. After transferal of proteins onto nitrocellulose filters, the blots were incubated with primary antibodies recognizing TJ proteins or RBPs; after incubations with secondary antibodies, immunocomplexes were visualized by using chemiluminescence.

Isolation of nuclear and cytoplasmic RNA

Nuclear and cytoplasmic RNA fractions from Caco-2 cells were isolated and purified with the SurePrep Nuclear/Cytoplasmic RNA Purification Kit from Fisher Bioreagents (Fair Lawn, NJ), following the manufacturer's instructions. Briefly, after lysis solution was added, whole-cell lysate was transferred and centrifuged at 17,000 × *g* for 3 min. The supernatant containing cytoplasmic RNA and the pellet containing nuclear RNA were saved separately and then mixed with the binding solution. After addition of ethanol, the mixtures were applied onto a spin column and centrifuged at 17,000 × *g* for 1 min, and then RNA was eluted. *Gapdh* mRNA levels were measured as an internal control for normalization. To assess any cross-contamination between cytoplasmic and nuclear fractions, the levels of β-tubulin (a specific cytoplasmic protein marker) and lamin B (a nuclear protein marker) were examined in the two fractions (Zou *et al.*, 2006).

Analysis of newly translated protein and polysome analysis

De novo synthesis of nascent TJ proteins was detected by a Click-IT Protein Analysis Detection Kit (Life Technologies, Grand Island, NY) and performed following the manufacturer's instructions. Briefly, cells were incubated in methionine-free medium and then exposed to AHA. After mixing cell lysates with the reaction buffer containing biotin/alkyne reagent and $CuSO_4$ for 20 min, the biotin-alkyne/azide–modified protein complex was pulled down using paramagnetic streptavidin-conjugated Dynabeads. The pull-down material was resolved by 10% SDS–PAGE and analyzed by Western immunoblotting analysis using the antibody against TJ proteins or GAPDH.

Polysome analysis was performed as described (Xiao *et al.*, 2013). Briefly, cells at ~70% confluence were incubated for 15 min in 0.1 mg/ml cycloheximide and then lifted by scraping in 1 ml of polysome extraction lysis buffer and lysed on ice for 10 min. Nuclei were pelleted, and the resulting supernatant was fractionated through a 15–60% linear sucrose gradient to fractionate cytoplasmic components according to their molecular weight. The eluted fractions were prepared with a fraction collector (Brandel, Gaithersburg, MD), and their quality was monitored at 254 nm using a UV-6 detector (ISCO, Louisville, KY). After RNA in each fraction was extracted, the levels of each individual mRNA were quantified by RT, followed by Q-PCR in each of the fractions.

Biotin-labeled *SPRY4-IT1* pull-down and RNP-IP assays

After biotin-labeled *SPRY4-IT1* was incubated with cytoplasmic proteins at room temperature for 1 h, the mixture was mixed with streptavidin-Dynal beads and incubated at 4°C on a rotator overnight. After the beads were washed thoroughly, the beads-bound RNA was isolated and subjected to RT, followed by Q-PCR analysis. To examine association of *SPRY4-IT1* with RBPs, levels of HuR and other proteins in the pull-down material were assessed after cytoplasmic lysates were incubated with biotinylated *SPRY4-IT1*.

To assess the association of endogenous HuR with endogenous TJ mRNAs or *SPRY4-IT1*, IP of RNP complexes was performed as described (Yu *et al.*, 2011). Twenty million cells were collected per sample, and lysates were used for IP for 4 h at room temperature in the presence of excess (30 μg) IP antibody (IgG, or anti-HuR). RNA in IP materials was used in RT, followed by PCR and Q-PCR analysis to detect the presence of TJ and *Gapdh* mRNAs.

RNA-FISH assay

The RNA-FISH assay was performed with the ISH Optimization Kit from Exiqon (Vedbaek, Denmark) as described (Elmen *et al.*, 2008). Briefly, the mucosa was fixed with 4% fresh paraformaldehyde overnight and embedded in paraffin for sections. The slides were

deparaffinized and then incubated with proteinase-K. After washes with PBS, the slides were dehydrated and hybridized with 25 nM fluorescent locked nucleic acid (LNA) probe for 1 h at 60°C. The slides were washed with saline sodium citrate buffer and PBS, covered with coverslides, and then processed using a Zeiss confocal microscope (Zeiss, Jena, Germany).

Measurements of gut epithelial barrier function

The epithelial barrier function in vitro was examined by paracellular tracer flux assays using a 12-well Transwell plate (surface area, 1.12 cm^2) as described (Guo *et al.*, 2003; Yu *et al.*, 2013). FITC-dextran (70 kDa; Sigma-Aldrich), a membrane-impermeable molecule, served as the paracellular tracer and was added to the apical bathing wells. The basal bathing well had no added tracers and contained the same flux assay medium as in the apical compartment. All flux assays were performed at 37°C, and the basal medium was collected 2 h after addition of the FITC-dextran. The concentration of the FITC-dextran in the basal medium was determined using a fluorescence plate reader with an excitation wavelength at 490 nm and an emission wavelength of 530 nm. TEER was measured with an epithelial voltmeter under open-circuit conditions (WPI, Sarasota, FL) as described (Yu *et al.*, 2013), and the TEER of all monolayers was normalized to that of control monolayers in the same experiment.

Gut permeability in vivo was determined by examining the appearance in blood of FITC-dextran administered by gavage as described (Furuta *et al.*, 2001). Briefly, mice were gavaged with FITC-dextran at a dose of 60 mg/100 g wt at 4 h before harvest. Blood sample was collected by cardiac puncture. The serum concentration of the FITC-dextran was determined using a fluorescence plate reader as described.

Surgical procedures

CLP was performed as described previously (Hubbard *et al.*, 2005). Mice were anesthetized by Nembutal (5.5 mg/100 g wt, intraperitoneally), and a midline abdominal incision was performed. The distal portion of the cecum (1 cm) was ligated with 5-0 silk suture. The ligated cecum was then punctured with a 25-gauge needle and slightly compressed with an applicator until a small amount of stool appeared. In sham-operated animals, the cecum was manipulated but without ligation and puncture and placed back in the peritoneum. The incision was closed using a two-layer procedure: 5-0 silk suture on the muscle layer and the skin, respectively. Mice received 1 ml of saline intraperitoneally for fluid resuscitation at the time of closure and 0.1 mg/100 g wt Buprenex subcutaneously four times at 12-h intervals to minimize distress.

Statistics

Values are means ± SEM from three to six samples. Autoradiographic results were repeated three times. The significance of the difference between means was determined by analysis of variance. Level of significance was determined by Duncan's multiple-range test (Harter, 1960).

ACKNOWLEDGMENTS

This work is supported by Merit Review Awards (to J.Y.W. and J.N.R.) from the U.S. Department of Veterans Affairs, grants from the National Institutes of Health (DK57819, DK61972, and DK68491 to J.Y.W.), and funding from the National Institute on Aging–Intramural Research Program, National Institutes of Health (to M.G.). J.Y.W. is a Senior Research Career Scientist, Biomedical Laboratory Research and Development Service, U.S. Department of Veterans Affairs.

REFERENCES

Abdelmohsen K, Panda AC, Kang MJ, Guo R, Kim J, Grammatikakis I, Yoon JH, Dudekula DB, Noh JH, Yang X, *et al.* (2014). 7SL RNA represses p53 translation by competing with HuR. Nucleic Acids Res 42, 10099–10111.

Batista PJ, Chang HY (2013). Long noncoding RNAs: cellular address codes in development and disease. Cell 152, 1298–1307.

Cao S, Xiao L, Rao JN, Zou T, Liu L, Zhang D, Turner DJ, Gorospe M, Wang JY (2014). Inhibition of Smurf2 translation by miR-322/503 modulates TGF-β/Smad2 signaling and intestinal epithelial homeostasis. Mol Biol Cell 25, 1234–1243.

Carter SR, Zahs A, Palmer JL, Wang L, Ramirez L, Gamelli RL, Kovacs EJ (2013). Intestinal barrier disruption as a cause of mortality in combined radiation and burn injury. Shock 40, 281–289.

Chen J, Xiao L, Rao JN, Zou T, Liu L, Bellavance E, Gorospe M, Wang JY (2008). JunD represses transcription and translation of the tight junction protein zona occludens-1 modulating intestinal epithelial barrier function. Mol Biol Cell 19, 3701–3712.

Cui YH, Xiao L, Rao JN, Zou T, Liu L, Chen Y, Turner DJ, Gorospe M, Wang JY (2011). miR-503 represses CUG-binding protein 1 translation by recruiting CUGBP1 mRNA to processing bodies. Mol Biol Cell 23, 151–162.

Elmen J, Lindow M, Schutz S, Lawrence M, Petri A, Obad S, Lindholm M, Hedtjarn M, Hansen HF (2008). LNA-mediated microRNA silencing in non-human primates. Nature 452, 896–899.

Feng SY, Dong CG, Wu WK, Wang XJ, Qiao J, Shao JF (2012). Lentiviral expression of anti-microRNAs targeting miR-27a inhibits proliferation and invasiveness of U87 glioma cells. Mol Med Rep 6, 275–281.

Furuse M, Izumi Y, Oda Y, Higashi T, Iwamoto N (2014). Molecular organization of tricellular tight junctions. Tissue Barriers 2, e28960.

Furuta GT, Turner JR, Taylor CT, Hershberg RM, Comerford K, Narravula S, Podolsky DK, Colgan SP (2001). Hypoxia-inducible factor 1-dependent induction of intestinal trefoil factor protects barrier function during hypoxia. J Exp Med 193, 1027–1034.

Guo X, Rao JN, Liu L, Zou TT, Turner DJ, Bass BL, Wang JY (2003). Regulation of adherens junctions and epithelial paracellular permeability: a novel function for polyamines. Am J Physiol 285, C1174–C1187.

Harter JL (1960). Critical values for Duncan's new multiple range tests. Biometric 16, 671–685.

Hubbard WJ, Choudhry M, Schwacha MG, Kerby JD, Rue LW 3rd, Bland KI, Chaudry IH (2005). Cecal ligation and puncture. Shock 24(Suppl 1), 52–57.

Ingolia NT, Brar GA, Rouskin S, McGeachy AM, Weissman JS (2012). The ribosome profiling strategy for monitoring translation in vivo by deep sequencing of ribosome-protected mRNA fragments. Nat Protoc 7, 1534–1550.

Khaitan D, Dinger ME, Mazar J, Crawford J, Smith MA, Mattick JS, Perera RJ (2011). The melanoma-upregulated long noncoding RNA SPRY4-IT1 modulates apoptosis and invasion. Cancer Res 71, 3852–3862.

Kim HH, Kuwano Y, Srikantan S, Lee EK, Martindale JL, Gorospe M (2009). HuR recruits let-7/RISC to repress c-Myc expression. Genes Dev 23, 1743–1748.

Liu L, Christodoulou-Vafeiadou E, Rao JN, Zou T, Xiao L, Chung HK, Yang H, Gorospe M, Kontoyiannis D, Wang JY (2014). RNA-binding protein HuR promotes growth of small intestinal mucosa by activating the Wnt signaling pathway. Mol Biol Cell 25, 3308–3318.

Liu L, Ouyang M, Rao JN, Zou T, Xiao L, Chung HK, Wu J, Donahue JM, Gorospe M, Wang JY (2015). Competition between RNA-binding proteins CELF1 and HuR modulates MYC translation and intestinal epithelium renewal. Mol Biol Cell 26, 1797–1810.

Liu L, Rao JN, Zou T, Xiao L, Wang PY, Turner DJ, Gorospe M, Wang JY (2009). Polyamines regulate c-Myc translation through Chk2-dependent HuR phosphorylation. Mol Biol Cell 20, 4885–4898.

Liu X, Li D, Zhang W, Guo M, Zhan Q (2012). Long non-coding RNA gadd7 interacts with TDP-43 and regulates Cdk6 mRNA decay. EMBO J 31, 4415–4427.

Mattick JS, Makunin IV (2006). Non-coding RNA. Hum Mol Genet 15(Spec No 1), R17–R29.

Mazar J, Zhao W, Khalil AM, Lee B, Shelley J, Govindarajan SS, Yamamoto F, Ratnam M, Aftab MN, Collins S, *et al.* (2014). The functional characterization of long noncoding RNA SPRY4-IT1 in human melanoma cells. Oncotarget 5, 8959–8969.

Mendell JT, Olson EN (2012). MicroRNAs in stress signaling and human disease. Cell 148, 1172–1187.

Mosenthal AC, Xu D, Deitch EA (2002). Elemental and intravenous total parenteral nutrition diet-induced gut barrier failure is intestinal site specific and can be prevented by feeding nonfermentable fiber. Crit Care Med 30, 396–402.

Mukherjee N, Corcoran DL, Nusbaum JD, Reid DW, Georgiev S, Hafner M, Ascano M Jr, Tuschl T, Ohler U, Keene JD (2011). Integrative regulatory mapping indicates that the RNA-binding protein HuR couples pre-mRNA processing and mRNA stability. Mol Cell 43, 327–339.

Nagatake T, Fujita H, Minato N, HamazakiY (2014). Enteroendocrine cells are specifically marked by cell surface expression of claudin-4 in mouse small intestine. PLoS One 9, e90638.

Ota T, Suzuki Y, Nishikawa T, Otsuki T, Sugiyama T, Irie R, Wakamatsu A, Hayashi K, Sato H, Nagai K, *et al.* (2004). Complete sequencing and characterization of 21,243 full-length human cDNAs. Nat Genet 36, 40–45.

Ponting CP, Oliver PL, Reik W (2009). Evolution and functions of long noncoding RNAs. Cell 136, 629–641.

Scherr M, Venturini L, Battmer K, Schaller-Schoenitz M, Schaefer D, Dallmann I, Ganser A, Eder M (2007). Lentivirus-mediated antagomir expression for specific inhibition of miRNA function. Nucleic Acids Res 35, e149.

Schneeberger EE, Lynch RD (2004). The tight junction: a multifunctional complex. Am J Physiol 286, C1213–C1228.

Sharma A, Bhat AA, Krishnan M, Singh AB, Dhawan P (2013). Trichostatin-A modulates claudin-1 mRNA stability through the modulation of Hu antigen R and tristetraprolin in colon cancer cells. Carcinogenesis 34, 2610–2621.

Shi Y, Li J, Liu Y, Ding J, Fan Y, Tian Y, Wang L, Lian Y, Wang K, Shu Y (2015). The long noncoding RNA SPRY4-IT1 increases the proliferation of human breast cancer cells by upregulating ZNF703 expression. Mol Cancer 14, 51.

Srikantan S, Gorospe M (2012). HuR function in disease. Front Biosci 17, 189–205.

Srikantan S, Tominaga K, Gorospe M (2012). Functional interplay between RNA-binding protein HuR and microRNAs. Curr Protein Pept Sci 13, 372–379.

Takahashi K, Yan I, Haga H, Patel T (2014). Long noncoding RNA in liver diseases. Hepatology 60, 744–753.

Terahara K, Yoshida M, Igarashi O, Nochi T, Pontes GS, Hase K, Ohno H, Kurokawa S, Mejima M, Takayama N, *et al.* (2008). Comprehensive gene expression profiling of Peyer's patch M cells, villous M-like cells, and intestinal epithelial cells. J Immunol 180, 7840–7846.

Tsai MC, Spitale RC, Chang HY (2011). Long intergenic noncoding RNAs: new links in cancer progression. Cancer Res 71, 3–7.

Turner JR (2009). Intestinal mucosal barrier function in health and disease. Nat Rev Immunol 9, 799–809.

Uchida S, Dimmeler S (2015). Long noncoding RNAs in cardiovascular diseases. Circ Res 116, 737–750.

Ulitsky I, Bartel DP (2013). lincRNAs: genomics, evolution, and mechanisms. Cell 154, 26–46.

Wang KC, Chang HY (2011). Molecular mechanisms of long noncoding RNAs. Mol Cell 43, 904–914.

Wapinski O, Chang HY (2011). Long noncoding RNAs and human disease. Trends Cell Biol 21, 354–361.

Xiao L, Rao JN, Zou T, Liu L, Cao S, Martindale JL, Su W, Chung HK, Gorospe M, Wang JY (2013). miR-29b represses intestinal mucosal growth by inhibiting translation of cyclin-dependent kinase 2. Mol Biol Cell 24, 3038–3046.

Xiao L, Wang JY (2014). RNA-binding proteins and microRNAs in gastrointestinal epithelial homeostasis and diseases. Curr Opin Pharmacol 19, 46–53.

Yang H, Rao JN, Wang JY (2014). Posttranscriptional regulation of intestinal epithelial tight junction barrier by RNA-binding proteins and microRNAs. Tissue Barriers 2, e28320.

Ye D, Guo S, Al-Sadi R, Ma TY (2011). MicroRNA regulation of intestinal epithelial tight junction permeability. Gastroenterology 141, 1323–1333.

Yoon JH, Abdelmohsen K, Srikantan S, Yang X, Martindale JL, De S, Huarte M, Zhan M, Becker KG, Gorospe M (2012). LincRNA-p21 suppresses target mRNA translation. Mol Cell 47, 648–655.

Yu TX, Rao JN, Zou T, Liu L, Xiao L, Ouyang M, Cao S, Gorospe M, Wang JY (2013). Competitive binding of CUGBP1 and HuR to occludin mRNA controls its translation and modulates epithelial barrier function. Mol Biol Cell 24, 85–99.

Yu TX, Wang PY, Rao JN, Zou T, Liu L, Xiao L, Gorospe M, Wang JY (2011). Chk2-dependent HuR phosphorylation regulates occludin mRNA translation and epithelial barrier function. Nucleic Acids Res 39, 8472–8487.

Zhang J, Yuan C, Hua G, Tong R, Luo X, Ying Z (2010). Early gut barrier dysfunction in patients with severe acute pancreatitis: attenuated by continuous blood purification treatment. Int J Artif Organs 33, 706–715.

Zhou Q, Costinean S, Croce CM, Brasier AR, Merwat S, Larson SA, Basra S, Verne GN (2015). microRNA-29 targets nuclear factor-κB-repressing factor and claudin 1 to increase intestinal permeability. Gastroenterology 148, 158–169.

Zhuang R, Rao JN, Zou T, Liu L, Xiao L, Cao S, Hansraj NZ, Gorospe M, Wang JY (2013). miR-195 competes with HuR to modulate stim1 mRNA stability and regulate cell migration. Nucleic Acids Res 41, 7905–7919.

Zou T, Mazan-Mamczarz K, Rao JN, Liu L, Marasa BS, Zhang AH, Xiao L, Pullmann R, Gorospe M, Wang JY (2006). Polyamine depletion increases cytoplasmic levels of RNA-binding protein HuR leading to stabilization of nucleophosmin and p53 mRNAs. J Biol Chem 281, 19387–19394.

Zou T, Rao JN, Liu L, Xiao L, Chung HK, Li Y, Chen G, Gorospe M, Wang JY (2015). JunD enhances miR-29b levels transcriptionally and post-transcriptionally to inhibit proliferation of intestinal epithelial cells. Am J Physiol 308, C813–C824.

Zou T, Rao JN, Liu L, Xiao L, Yu TX, Jiang P, Gorospe M, Wang JY (2010). Polyamines regulate the stability of JunD mRNA by modulating the competitive binding of its 3′ untranslated region to HuR and AUF1. Mol Cell Biol 30, 5021–5032.